MDPI

Article

Anaerobic Digestion and Hot Water Pretreatment of Tropically Grown C$_4$ Energy Grasses: Mass, Carbon, and Energy Conversions from Field Biomass to Fuels

Jon M. Wells [1],*, Susan E. Crow [1], Samir Kumar Khanal [2], Scott Turn [3], Andrew Hashimoto [2], Jim Kiniry [4] and Norman Meki [5]

1   Department of Natural Resources and Environmental Management, University of Hawaii at Manoa, 1910 East West Rd, Honolulu, HI 96822, USA; crows@hawaii.edu
2   Department of Molecular Biosciences and Bioengineering, University of Hawaii at Manoa, 1955 East West Rd, Honolulu, HI 96822, USA; khanal@hawaii.edu (S.K.K.); andrew.hashimoto@hawaii.edu (A.H.)
3   Hawaii Natural Energy Institute, University of Hawaii at Manoa, 1680 East West Rd, Honolulu, HI 96822, USA; sturn@hawaii.edu
4   Grassland Soil and Water Research Laboratory, USDA Agricultural Research Service, 808 East Blackland Rd, Temple, TX 76502, USA; jim.kiniry@usda.gov
5   Texas A&M AgriLife Research, Blackland Research and Extension, 808 East Blackland Rd, Temple, TX 76502, USA; nmeki@brc.tamus.edu
*   Correspondence: jonwells@hawaii.edu

Abstract: The efficacy of C$_4$ grasses as feedstocks for liquid fuel production and their climate mitigation potential remain unresolved in the tropics. To identify highly convertible C$_4$ grasses, we measured final fuels and postprocess biomass produced in two laboratory-scale conversion pathways across 12 species and varieties within the *Poaceae* (grass) family. Total mass, carbon, and energy in final fuels and postprocess biomass were assessed based on field mass and area-based production. Two lignocellulosic processes were investigated: (1) anaerobic digestion (AD) to methane and (2) hot water pretreatment and enzymatic hydrolysis (HWP-EH) to ethanol. We found AD converted lignocellulose to methane more efficiently in terms of carbon and energy compared to ethanol production using HWP-EH, although improvements to and the optimization of each process could change these contrasts. The resulting data provide design limitations for agricultural production and biorefinery systems that regulate these systems as net carbon sources or sinks to the atmosphere. Median carbon recovery in final fuels and postprocess biomass from the studied C$_4$ grasses were ~5 Mg C ha^{-1} year^{-1} for both methane and ethanol, while median energy recovery was ~200 MJ ha^{-1} year^{-1} for ethanol and ~275 MJ ha^{-1} year^{-1} for methane. The highest carbon and energy recovery from lignocellulose was achieved during methane production from a sugarcane hybrid called energycane, with ~10 Mg C ha^{-1} year^{-1} and ~450 MJ ha^{-1} year^{-1} of carbon and energy recovered, respectively, from fuels and post-process biomass combined. Carbon and energy recovery during ethanol production was also highest for energycane, with ~9 Mg C ha^{-1} year^{-1} and ~350 MJ ha^{-1} year^{-1} of carbon and energy recovered in fuels and postprocess biomass combined. Although several process streams remain unresolved, agricultural production and conversion of C$_4$ grasses must operate within these carbon and energy limitations for biofuel and bioenergy production to be an atmospheric carbon sink.

Keywords: tropical; C$_4$ grasses; lignocellulose; anaerobic digestion; hot water pretreatment; biofuels

1. Introduction

Agricultural systems must be sustainably intensified to provide adequate food, fuel, and fiber to support projected increases in global energy and food demand [1,2]. Conservation agricultural practices, in the form of zero or minimal tillage, residue management,

and plant cover, can positively affect the carbon (C) cycle and advance sustainable development [3]. Belowground C allocation and total soil organic carbon (SOC) in temperate and (sub)tropical systems can also be improved through transitions to perennial bioenergy grasses from conventionally managed crops [4]. Specifically, conversion of marginal croplands and areas of low C storage potential to high biomass-producing, deep-rooted, bioenergy grasses under conservation agriculture can improve climate mitigation potential [5–7], while the produced bioenergy can directly offset fossil fuels. However, there is high uncertainty in the net amount of C and energy harvestable from these systems based on land use and management combinations [8], especially in the tropics and across large spatial scales [9], making it uncertain if agricultural bioenergy production can be established as net C sinks to the atmosphere.

In the tropics, limited data impede our understanding of how fast-growing grass feedstocks and year-round growth climates relate to the conversion efficiencies of energy and C in these crops. Literature comparisons of multiple potential C_4 energy grasses through contrasting lignocellulosic conversion pathways in the tropics are also limited [10]. Thus, the tropical application of growth and conversion is an important knowledge gap that inhibits the practical use of many potential C_4 grasses for biofuels in these areas. Furthermore, lignocellulose can vary widely across tropically grown C_4 grasses, with total lignin and lignin chemical composition changing across plant parts and within species and varieties based on environmental conditions [11,12]. As changing biomass composition can affect conversion, life cycle assessments (LCAs) of tropical bioenergy production require further C and energy assessments to evaluate the efficacy of C_4 grasses as climate mitigation tools.

In Hawaii specifically, legislative mandates for renewable energy [13,14] have positioned the state to ramp up biomass production for energy; but first, there must be confidence that these production systems are not, in fact, net C sources [15]. Tracking C throughout the production and conversion of these grasses can inform the C neutrality of these systems [16], from C offsets in soils and C captured in biomass to final C values in fuels. However, despite the establishment of a diverse range of pretreatment/conversion options [17], there is still much debate and continued research into the top-performing feedstocks and conversion processes for tropical liquid fuel production [10], due, in part, to the many unknowns in bioenergy production and conversion systems [2]. Methods to evaluate feedstock production and conversion efficacy can also change based on biases in LCAs, including the treatment of land-use change (both direct and indirect), fossil fuel reference systems, allocation of substrates to variable conversion products, and where system boundaries are drawn [16].

In this study, C and energy conversion efficiencies are explored across several potential bioenergy grass feedstocks and two conversion pathways. The purpose of our work is to identify crop-conversion combinations that best support both environmental and energy sustainability goals in terms of C and energy recovered in fuels and postprocess biomass. Two potential conversion pathways were selected: (1) anaerobic digestion (AD) and (2) hot water pretreatment (HWP) followed by enzymatic hydrolysis (EH). These two conversion processes were chosen to contrast the enzymatic hydrolysis of structural lignocellulose—the hardest energy to access from plant-based polymers. C and energy were quantified in field biomass, intermediate products, final fuels, and postprocess biomass, with the expectation that more intensive HWP would allow us to access more structural sugars and create higher C and energy conversion efficiency.

2. Materials and Methods

2.1. C_4 Grasses

Twelve C_4 grasses were tested for energy and C conversion efficiencies (Table 1), including three varieties of napiergrass (*Pennisetum purpureum*), three varieties of sugarcane (*Saccharum officinarum*), three sugarcane hybrids called energycane (*Saccharum officinarum x Saccharum robustum*), maize (*Zea mays* L.), sorghum (*Sorghum bicolor* (L.) Moench), and

sudex (*Sorghum bicolor x S. bicolor var. Sudanese*). Napiergrass, sugarcane, and energycane were grown in replicated field trials, as described by Youkhana et al. [18]. Maize, sorghum, and sudex were grown in adjacent unreplicated field trials to produce example biomass for conversion. Napiergrass, sugarcane, and energycane yields were measured in the field, while yields for maize, sorghum, and sudex were estimated from literature. Approximately 10–20 full stalks of each grass were randomly collected during ratoon harvest in September 2015 to provide ~2 kg of dry biomass per crop. Experiments were conducted on biomass from composited samples consisting of material from plot replicates combined in equal mass from replicated field trials. Conversion through both AD and HWP-EH was then performed in triplicate from composited samples.

Table 1. C_4 grasses and their yields in Mg ha^{-1} year^{-1}.

C_4 Grasses	Taxonomy	Variety	Yield (Mg ha^{-1} Year^{-1})
Maize	*Zea mays*		21.1 [a]
Sorghum	*Sorghum bicolor*		21.3 [b]
Sudex	*Sorghum bicolor x S. bicolor var. sudanese*		26.4 [c]
		255	19.8
		Green	24.2
		Purple	19.3
Energycane	*Saccharum officinarum x Saccharum robustum*	EC6081	38.4
		EC6136	29.2
		EC9271	31.5
		SC3792	24.6
		SC5867	25.5
		SC7052	35.8

[a] [19], [b] [10], [c] [20].

2.2. Anaerobic Digestion

Randomly sampled full stalks of each grass were fed through a 3-inch chipper/shredder (Bearcat, SC3306, Briggs & Stratton, Wauwatosa, WI, USA) before being air-dried on large trays in a ventilated greenhouse at approximately 35–40 °C. As drying progressed, sub-samples were taken and dried at 105 °C until biomass was below 10% moisture content. Biomass was then transported from Maui to Oahu for size-processing to 2 mm using a Wiley mill (Thomas Scientific, Swedesboro, NJ, USA). Biomass subsamples were measured for moisture content before use. Mass was accounted for by dry weight equivalents for all experiments. Field replicates were combined in equal mass to a single composite sample before conversion to fuels. Experiments with more coarsely ground material and at larger scales will be important future work, but both are outside the scope of this bench-scale research. For AD, water-extractable substrates were removed from all crops using distilled water and a Soxhlet extractor until extraction water was clear. Biomass samples subjected to AD were thus comparable to bagasse, with freely accessible sugars removed before use. This was done to focus on the conversion of structural lignocellulose without interference from water-extractable plant sugars.

The inoculum used for AD was prepared from cattle manure, similar to Surendra and Khanal [21]. Briefly, a 20 L inoculum reactor was maintained at neutral pH and the mesophilic temperature of 37 °C until the daily rate of methane production was negligible. Once methane production ceased (up to 30 days after start), the inoculum was sieved through a No.8 US ASTM standard sieve (nominal opening of 2.36 mm), with the liquid passing through the sieve collected as inoculum. AD digestion was performed in 500 mL Erlenmeyer flasks with screw caps that contained one septa port and one closable valve to a 1 L Tedlar gas bag. Total solids (TS) and volatile solids (VS) of all grasses and inoculum were measured by oven drying samples before loss on ignition. A drying temperature of 105 °C was used for TS measurement, with samples then combusted at 550 °C. Remaining

ash was measured by weight, and VS was calculated by subtracting ash from dry matter, with ash comprising 4–9% of total field biomass. The AD process was conducted using a 1:1 substrate-to-inoculum ratio (VS basis) [21], while substrate loading was maintained at 2.5 g VS/250 mL working volume. To facilitate recapture of the digested substrate, a 2.5 g VS equivalent of water-extracted plant material was sealed in 37-micron mesh polyester bags before being submerged in inoculum. The 250 mL working volume of inoculum was created by diluting the equivalent of 2.5 g VS of sieved inoculum with distilled water.

Differences in inoculum batches were controlled by rep, with each replicate containing all species and an inoculum control run concurrently on a single shaker for 30 days. The shaker and bottles were maintained at 37 °C within a Caron environmental chamber. Biogas volume was measured by gas mill, with CH_4, CO_2, N_2, and O_2 concentrations measured by gas chromatography (Clarus 500 GC, PerkinElemer, Waltham, MA, USA) using a thermal conductivity detector. The mass of produced CH_4 was calculated using the gas law and standard ambient temperature and pressure (SATP), which matched measurement conditions. After digestion, the plant sample bags were removed from the inoculum, rinsed until only plant material was visible, and dried at 43 °C. A further subsample was dried at 105 °C to calculate moisture content and remaining biomass after digestion.

2.3. Hot Water Pretreatment and Enzymatic Hydrolysis

Hot water pretreatment was conducted on the same composite field samples used in AD. Instead of first removing water-extractives like AD, the biomass was subjected to HWP, which is known to remove water-extractable sugars, most hemicelluloses, and lesser amounts of other structural lignocellulose [22–26]. HWP was conducted in a custom-made 3 L high-pressure vessel (High Pressure Equipment Company, Erie, PA, USA) milled from stainless steel and designed for pressures up to 3000 psi. Temperature was controlled using a thermal probe, digital temperature controller, and two 1500-watt constant current heating strips.

Experimental conditions were chosen to optimize enzymatic hydrolysis of washed lignocellulose (i.e., hot water pretreated biomass) to glucose based on combinations of temperature, biomass loading, and enzyme loading of purple napiergrass and energy-cane [27]. Final conditions used across all grasses were 220 °C, a temperature ramp of 1 °C min^{-1}, and a 10-min hold time. The 3 L high-pressure vessel was loaded with 2.5 L of deionized (DI) water and a dry equivalent of 250 g field biomass (10% w/v loading). The pressure at hold time was approximately 420 psi—conditions under which water would remain almost entirely in the liquid phase. It was found that above 200 °C, furfural and other inhibitory compounds increased, while structural sugar released during enzymatic hydrolysis reached a maximum at around 220 °C [27]. After hot water pretreatment, plant material was captured on a 250 μm sieve, rinsed 3 times with DI water to ensure that inhibitory compounds did not interfere with enzymatic hydrolysis, and hand-squeezed before rapid moisture determination using a moisture analyzer (M5, Ohaus, Parsippany, NJ, USA).

Enzymatic hydrolysis was performed at 10% w/v loading using a dry equivalent of 25 g of HWP pretreated biomass in a working volume of 250 mL within a 500 mL Erlenmeyer flask. Concentrated sodium azide (0.5 mL) and 4 mL (~13 mg protein/g biomass) of a mixture of endo- and beta-glucosidases (Accellerase® 1500, Dupont™, Wilmington, DE, USA) were added to 125 mL of 0.1 M sodium citrate buffer adjusted to pH 4.8, with the remaining 250 mL working volume made up by water. The Accellerase® 1500 enzyme had a protein content of 82 mg/mL [28] and a filter paper activity (FPU) of 0.5 FPU/mg protein [29,30], with an optimal pH range of 4.0–5.0 and an optimal temperature range of 50–65 °C, based on DuPont™ correspondence. Erlenmeyer flasks containing the enzyme–substrate slurry were shaken on a 1-inch orbital shaker (Excella E5 Platform Shaker, New Brunswick Scientific, Edison, NJ, USA) at 200 rpm for 72 h at 50 °C. Extracted structural glucose was measured by HPLC (Alliance 2695 HPLC, Waters, Milford, MA, USA) and compared to an external glucose calibration curve. Enzyme-extracted glucose from the

solid biomass fraction recovered after HWP was used to calculate ethanol production using literature-based conversion efficiencies, as described in the following section.

2.4. Mass, Carbon, and Energy Calculations

Process conditions for AD and HWP-EH were designed to maximize comparability between the two procedures in terms of structural lignocellulose conversion to fuel. Overall, the production of methane during AD and ethanol from sugars extracted by HWP-EH are quite different based on the process steps, resulting in final fuels. However, the two processes share a key underlying similarity—the hydrolytic breakdown of structural sugars for energy, which is a major constraint on process efficiency. Thus, AD conducted here can be viewed as a biologically driven enzymatic process accessing structural lignocellulose. In contrast, HWP-EH is an energetic process where nonstructural biomass and a portion of structural lignocellulose, especially hemicelluloses, are removed by thermohydrolysis to improve enzymatic saccharification. With this framing, the two energy pathways were investigated for the production of final fuels from structural lignocellulose, specifically. C and energy of the initial biomass, washed structural lignocellulose, and the remaining postprocess biomass were measured by elemental analysis (EA; LECO, CHNS 628 Elemental Analyzer, St. Joseph, MI, USA) and bomb calorimetry (6200 Bomb Calorimeter, Parr Instrument Company, Moline, IL, USA).

Glucose extracted from each crop during HWP-EH was scaled to ethanol as a current industry standard, with many literature comparisons and immediate application. The literature shows as high as 96% bench-scale ethanol efficiency from glucose using cocultures [31], while industrial-scale production of ethanol from sugarcane in Brazil is currently trying to improve from ~83% to a goal efficiency of 90% using process optimization [32]. To keep ethanol production reasonable, considering the current large-scale industrial limitations, 85% efficiency of the theoretical ethanol yield from glucose was used for pathway comparisons, which can be updated as industrial efficiency improves. The stoichiometry of ethanol production from glucose is:

$$C_6H_{12}O_6 \rightarrow 2C_2H_6O + 2CO_2 \tag{1}$$
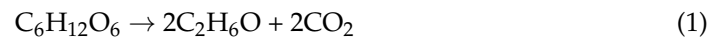
where the mass efficiency of glucose to ethanol can be calculated as $92.14/180.16 \cong 51\%$. The mass of water gained by glucose during hydrolysis from cellulose was accounted for using the hydrolysis reaction:

$$2C_6H_{10}O_5 + 2H_2O \rightarrow 2C_6H_{12}O_6 \tag{2}$$
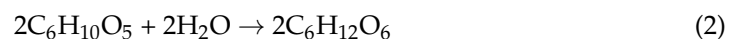
where the mass contribution of cellulose to hydrolyzed glucose is $324.28/360.32 \cong 90\%$. This leads to an overall calculation of ethanol produced from glucose extracted:

$$M_{glu} (H_c) (Y_{eth}) (E_{eth}) = M_{c,eth} \tag{3}$$

where M_{glu} is the proportion of glucose mass extracted from the HWP biomass, H_c is the contribution of biomass cellulose to the hydrolyzed glucose mass (90%), Y_{eth} is the theoretical yield of ethanol from glucose (51%), E_{eth} is the efficiency of ethanol from glucose during fermentation (85%), and $M_{c,eth}$ is the proportion of ethanol mass produced from the HWP biomass. In contrast, the proportion of methane produced during the conversion step ($M_{c,meth}$) can be calculated directly by dividing the mass of methane produced by the mass of washed biomass added to AD digestion bags.

Mass of fuel produced from conversion can be related back to field biomass by the proportion of mass recovered after HWP and washing before conversion, leading to final mass calculations from each fuel production pathway:

$$M_{hwp} (M_{c,eth}) = M_{f,eth} \tag{4}$$

$$M_{wash} (M_{c,meth}) = M_{f,meth} \tag{5}$$

where M_{hwp} and M_{wash} are the proportions of mass recovered after hot water pretreatment and washing of field biomass, respectively, and $M_{f,eth}$ and $M_{f,meth}$ are the final proportions of fuel mass produced from field biomass for ethanol and methane, respectively.

Fuel mass from field biomass can then be used to calculate the recovery of C in final fuels. The mass of C in ethanol and methane was 52.1% and 74.9%, respectively, which were multiplied by fuel mass to calculate C mass in the final fuels. The mass of C in fuels was then scaled to a percent of initial biomass C (i.e., C efficiency). Working with proportions makes C efficiency a simple calculation for each crop and pathway:

$$M_{f,eth} \; (C_{eth})/C_{field} = C_{eff,eth} \tag{6}$$

$$M_{f,meth} \; (C_{meth})/C_{field} = C_{eff,meth} \tag{7}$$

where C_{eth} is the C percent of ethanol (52.1%), C_{meth} is the C percent of methane (74.9%), C_{field} is the C percent of field biomass, and $C_{eff,eth}$ and $C_{eff,meth}$ are the final C efficiencies of ethanol and methane produced from field biomass, respectively.

Energy produced from field biomass was also calculated from the fuel mass produced. Specific energies of 26.8 and 55.6 MJ kg^{-1} were used for energy calculations of ethanol and methane production, respectively. The following equations were used for energy calculations:

$$M_{f,eth} \; (SE_{eth}) = E_{eth} \tag{8}$$

$$M_{f,meth} \; (SE_{meth}) = E_{meth} \tag{9}$$

where SE_{eth} and SE_{meth} are the specific energies of ethanol and methane, respectively, and E_{eth} and E_{meth} are the amounts of fuel produced per unit field biomass (i.e., MJ per kg of field biomass).

Similar to fuel calculations, the mass, C, and energy in postprocess biomass can be related back to field biomass and field C. The mass of postprocess biomass as a percentage of field mass was calculated using the following equations:

$$M_{hwp} \; (M_{b,eth}) = M_{pp,eth} \tag{10}$$

$$M_{wash} \; (M_{b,meth}) = M_{pp,meth} \tag{11}$$

where $M_{b,eth}$ and $M_{b,meth}$ are the proportions of HWP and washed biomass that were recovered postprocess, while $M_{pp,eth}$ and $M_{pp,meth}$ are the proportions of field biomass that were recovered postprocess. Postprocess C was also related back to field C:

$$M_{pp,eth} \; (C_{b,eth})/C_{field} = C_{pp,eth} \tag{12}$$

$$M_{pp,meth} \; (C_{b,meth})/C_{field} = C_{pp,meth} \tag{13}$$

where $C_{b,eth}$ and $C_{b,meth}$ are the C percentages of postprocess biomass after ethanol and methane production, respectively, and $C_{pp,eth}$ and $C_{pp,meth}$ are the proportions of field C that were recovered in postprocess biomass. Finally, the energy of postprocess biomass was calculated using the following equations:

$$M_{pp,eth} \; (SE_{b,eth}) = E_{pp,eth} \tag{14}$$

$$M_{pp,meth} \; (SE_{b,meth}) = E_{pp,meth} \tag{15}$$

where $SE_{b,eth}$ and $SE_{b,meth}$ are the measured specific energies of postprocess biomass from each C_4 grass after ethanol and methane production, respectively, while $E_{pp,eth}$ and $E_{pp,meth}$ are the amounts of energy in postprocess biomass per unit field biomass. Final comparisons of mass, C, and energy in fuels and postprocess biomass were statistically analyzed in R [33] across grasses and pathways using two-way ANOVA, including an interaction term, followed by Tukey's posthoc contrasts ($p < 0.05$).

*2.5. Mass, Carbon, and Energy Yields by Harvest Area*

Mass, C, and energy in fuels and postprocess biomass were related to agricultural feedstock production area using field yield. Average field yield from each grass was multiplied by average mass, C, and energy in final fuels and postprocess biomass for both pathways. Statistical comparisons between the resulting area-based production yields are not possible as some of the grasses converted to fuels were not grown in replicated field trials. However, differences between the grasses were generally small compared to pathway contrasts and contrasts between final fuels and postprocess biomass. Simple summary statistics were, thus, calculated to represent typical mass, C, and energy responses across these C_4 grasses. Median, first, and third quantiles and 95% confidence intervals of mass, C, and energy generated in produced fuels and postprocess biomass were compared from both the HWP-EH and AD conversion pathways.

3. Results and Discussion

3.1. Washing Losses, Final Fuels, and Postprocess Biomass from Field

As expected, due to thermohydrolysis at 220 °C and 420 psi, biomass recovery after HWP was vastly reduced, with only 32–50% of field biomass recovered (Figure 1A), while the efficiency of enzymatic hydrolysis of lignocellulose after pretreatment was maximized. In contrast, biomass recovery after simple water washing was 60–88% of field biomass, reflecting losses of nonstructural biomass that include free sugars and other water-extractive plant cell components. Importantly, all data and comparisons are presented on a dry mass basis. Significant differences in recovery between HWP and simple water washing and across grasses are apparent by two-way ANOVA and Tukey's posthoc contrasts ($p < 0.05$). The difference between the washing procedures also suggests that up to 28–38% of biomass lost to the liquid fraction during HWP were hemicelluloses, among lesser losses of other structural compounds. During HWP, hemicelluloses are almost entirely removed from the solid biomass fraction [22–26] and converted to acids [34], such as acetic acid, and inhibitory products such as furfural and hydroxymethylfurfural in the liquid fraction as HWP temperatures increase [27]. Importantly, we focused on the solid fraction generated by HWP. Thus, acids and further inhibitory sugar breakdown products generated from free sugars and hemicellulose degradation in the liquid fraction are not considered here for fuel generation and will require further work to resolve as waste-to-resource streams [34]. Acetic acid, specifically, could be diverted for industrial chemical use and offset the 1.4–1.9 CO_2-eq kg^{-1} required for typical acetic acid synthesis [35].

The HWP and washing data show that each conversion process can access different structural lignocellulosic substrates. Our experimental HWP-EH process produced ethanol entirely from cellulose, while AD utilized microbially accessible hemicelluloses and cellulose structural substrates. As HWP conditions were chosen to maximize glucose recovery per mass of pretreated lignocellulose, the data highlight that a process step to access hemicelluloses before HWP could improve the energy outlook for lignocellulosic ethanol production. Accessing hemicelluloses could be accomplished by first performing AD, for example, or an initial lower temperature pretreatment [25] before more intensive HWP is performed. Further optimization of the HWP pretreatment process that concurrently maximizes enzyme accessibility to cellulose and retention of other energy-rich compounds, especially hemicelluloses, will modify current contrasts between the HWP-EH and AD pathways. Concurrent work in the literature has also highlighted that agitation during enzymatic hydrolysis, as used in this study, causes losses of enzymes at the air–liquid interface, meaning less agitation, longer reaction times, and amphiphilic additives could all improve the ethanol outlooks presented here [28]. Future work could also make the presented fuel values partially additive by using sequential AD and HWP-EH to first access hemicelluloses for methane production and then convert the remaining cellulose to liquid fuels.
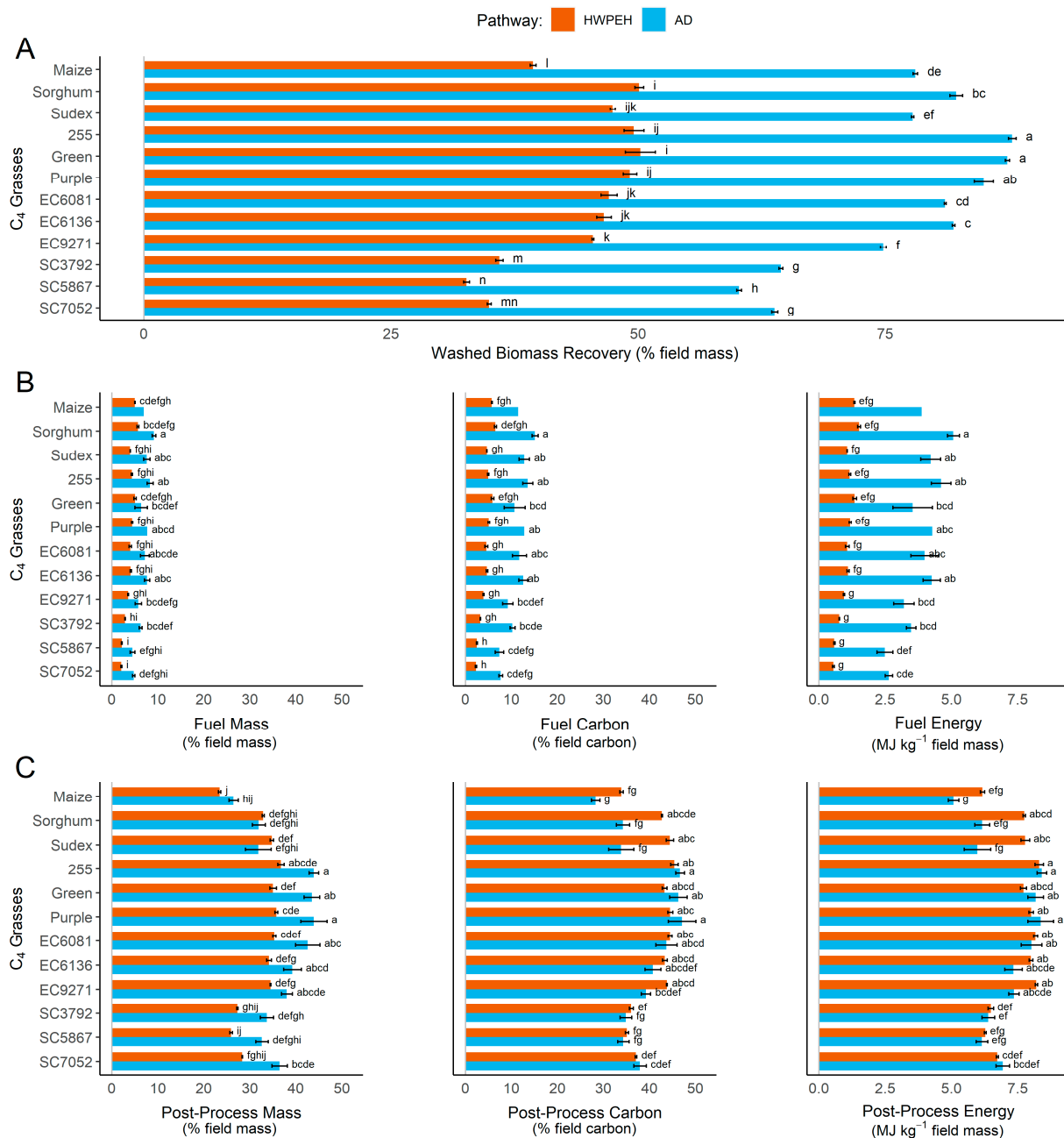
Figure 1. Recovery of structural lignocellulose, fuel mass, and postprocess biomass from field mass (% dry basis). Both the HWP-EH pathway, producing ethanol (orange), and the AD pathway, producing methane (blue), are shown. Comparative recovery of (**A**) biomass after HWP and water-washing, (**B**) fuel mass, fuel C, and fuel energy of ethanol and methane, and (**C**) postprocess biomass. Letters represent Tukey's posthoc contrasts of a two-way ANOVA ($p < 0.05$).

Fuel mass produced from each process showed significant Tukey's posthoc contrasts ($p < 0.05$) between pathways for most of the grasses studied (Figure 1B). However, there were few significant contrasts between grasses, with only the most and least convertible crops statistically separable. Sorghum had the most convertible structural lignocellulose while the least convertible grasses were SC7052 and SC5867 for ethanol and methane production, respectively. Across all C_4 grasses, 2–6% of field biomass was converted to ethanol by HWP-EH, while 4–9% of field biomass was converted to methane using AD. The higher C percent of methane (74.9% C) compared to ethanol (52.1% C) and the higher specific energy of methane (55.6 MJ kg^{-1}) compared to ethanol (26.8 MJ kg^{-1}) further amplified the differences between the two fuel pathways. Approximately 2–7% of C in

field biomass was recovered in ethanol compared to 7–15% of field C recovered in methane. In terms of energy, 0.5–1.5 MJ kg^{-1} of field biomass was produced as ethanol, while 2.5–5.0 MJ kg^{-1} of field biomass was produced as methane.

Postprocess biomass as a waste-to-resource stream was collected at the end of both HWP-EH and AD (Figure 1C). Green and purple napiergrass and SC7052 were the only grasses that had significantly higher postprocess biomass recovery in AD compared to HWP-EH, while pathway comparisons for all other grasses were not statistically separable. Within each conversion process, napiergrasses had significantly higher postprocess biomass recovery compared to sugarcane and maize, with all other grasses having intermediate values. Overall, a range of 23–37% of field biomass was recovered as postprocess biomass after ethanol production, with 26–44% of field biomass recovered in post-methane production. In contrast to fuels, postprocess biomass after HWP-EH had higher C (54–65% C) compared to postprocess biomass from methane production (46–49% C). The higher C concentration in postprocess biomass after HWP-EH also led to higher energy yields, where 21–26 MJ kg^{-1} postprocess biomass was recovered compared to 18–19 MJ kg^{-1} postprocess biomass after AD. C and energy recovered in postprocess biomass were only statistically different between pathways for sorghum and sudex. Overall, approximately 28–47% of field C was recovered in postprocess biomass after AD, while 34–45% of field C was recovered in postprocess biomass after HWP-EH. In contrast to fuels, energy recovery in postprocess biomass ranged from approximately 5.0–8.0 and 6.0–8.0 MJ kg^{-1} field biomass for AD and HWP-EH, respectively.

The data here are significant as they allow the estimation of mass, C, and energy contributions of lignocellulose to final fuels and postprocess biomass. With this information, it is possible to piece together systems that can best use mass, C, and energy across C$_4$ grasses and between HWP-EH and AD fuel processes. For example, proportions of recovered postprocess C could be allocated back to the soil as a C and nitrogen amendment. With approximately 1–2% of postprocess biomass measured as nitrogen, using postprocess biomass as a soil amendment could offset both fossil fuel and monetary costs associated with fertilizer [36]. Combustion of postprocess biomass could also increase overall energy harvest 2- to 5-fold from field biomass, depending on which process and grass are used. The sequential combination of AD and HWP-EH has further potential to minimize losses of hemicelluloses during HWP by first digesting hemicelluloses into methane. Outcomes from lignocellulose conversion can also be related to structural controls on conversion, such as lignin phenolic composition [11,37], which we are exploring in other work. Finally, we can also scale these comparisons to agricultural production areas using field yields to start answering questions related to production areas needed for tropical agricultural biorefinery systems.

3.2. Overall Mass, Carbon, and Energy per Hectare Across Crops and Pathways

Total mass, C, and energy for final fuel and postprocess biomass from each C$_4$ grass were related back to harvest area for both conversion pathways (Figure 2A). When related back to field area by tropical agricultural yields (Table 1), the 6081 variety of energycane produced the greatest mass, C, and energy in fuels and postprocess biomass for both pathways. Notably, these values are lignocellulose-specific and can be augmented based on how nonstructural sugars and starches are expected to be utilized, which has been well explored in the first-generation bioethanol production of maize and sugarcane [38,39]. Focusing on the utilization of lignocellulose and considering both produced fuels and postprocess biomass, EC6081 in the AD pathway produced ~20 Mg ha^{-1} year^{-1} of mass in fuels and postprocess biomass, with ~10 Mg ha^{-1} year^{-1} of C and ~450 MJ ha^{-1} year^{-1} of energy produced. In contrast, utilization of EC6081 in the HWP-EH pathway for ethanol generated ~15 Mg ha^{-1} year^{-1} of mass in fuels and postprocess biomass, with ~9 Mg ha^{-1} year^{-1} of C and ~350 MJ ha^{-1} year^{-1} of energy produced.
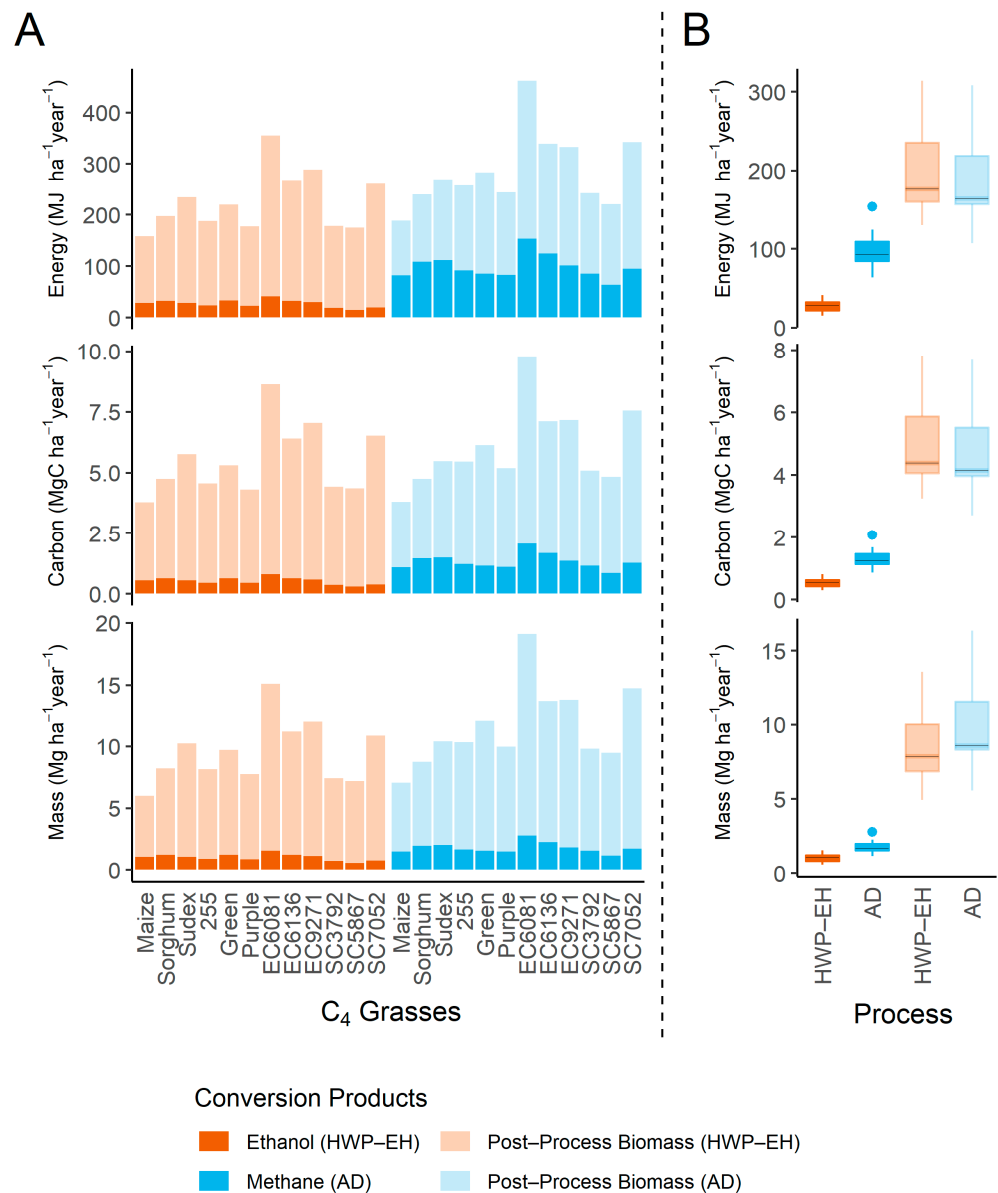
Figure 2. Mass, carbon, and energy content of generated fuels (dark) and postprocess biomass (light) by harvest area. Average yields of fuel and postprocess biomass were multiplied by average mass, carbon, and energy recovery after HWP-EH and AD (**A**). Yield data for maize, sorghum, and sudex were estimated by literature, while all other crop yields were measured in the field. Median, first, and third quantiles and 95% confidence intervals of C$_4$ grass response by pathway, fuel, and postprocess biomass in terms of mass, carbon, and energy are shown (**B**).

The final fuel mass was small in comparison to postprocess lignocellulose for all grasses in both the HWP-EH and AD fuel conversion pathways. The high C content of methane led to 16–31% of C recovered in methane vs. postprocess biomass using AD, with only 6–15% of C recovered in ethanol by HWP-EH. Similarly, the greater energy content in methane led to 27–45% of total energy recovered as methane across the grasses studied, while ethanol accounted for only 8–18% of total energy recovered. Again, ethanol mass from lignocellulose could be increased by process steps that better utilize hemicelluloses before HWP. However, the proportion of C and energy in fuels compared to postprocess biomass can only be improved by generating a fuel with a greater conversion efficiency and higher C and energy content than ethanol. Importantly, as our experimental HWP-EH process generated only glucose, other fuel values can be calculated from this glucose data

based on production efficiencies from other potentially more competitive second-generation liquid biofuels as the industry matures [40,41].

Summarizing the grasses by conversion pathway highlights that postprocess biomass utilization will be a key design aspect for biorefineries that aim to use similar crops and fuel conversion technologies (Figure 2B). Lignocellulose from grasses produced ~8 Mg ha^{-1} year^{-1} in postprocess biomass, while only 1–2 Mg ha^{-1} year^{-1} of fuels were generated. Approximately half of the postprocess biomass was C, with ~4 Mg ha^{-1} year^{-1} of C recovered after both the AD and HWP-EH conversion processes. As an important constraint, the combined total of C recovered in fuels and postprocess biomass will determine if an agricultural production and biorefinery system is a net source or sink of C to the atmosphere. Bioenergy production systems that utilize these C$_4$ grasses must be designed within the constraint of approximately 5 Mg ha^{-1} year^{-1} of C inputs for either pathway to create biofuels and bioenergy from postprocess biomass, with no net emissions to the atmosphere. Improved harvest management of C$_4$ grasses has also been demonstrated to rapidly increase SOC and could provide additional atmospheric C offsets [7]. Return of some fraction of postprocess biomass as a soil C and nitrogen amendment could also force the system towards a net C sink [36].

Agricultural production and biorefinery systems can also be energy-independent if growth and conversion of C$_4$ grasses to fuel can be achieved within ~275 MJ ha^{-1} year^{-1} using AD and ~200 MJ ha^{-1} year^{-1} for HWP-EH. In both cases, utilization of the energy remaining in postprocess biomass will be an important design consideration. Several process streams also remain unresolved, including C and energy losses during HWP as well as CO$_2$ and digestate created during methane production, which will need further investigation to improve the final climate mitigation potentials of these systems. Overall, the C and energy values of fuels and postprocess biomass inform the optimal use of lignocellulose in tropical agricultural bioenergy production systems, with the integration of these values into LCA and system-level analyses of C and energy flow planned in future work.

4. Conclusions

In terms of both C and energy from field biomass, AD converted lignocellulose into methane more efficiently than HWP-EH converted lignocellulose into ethanol. Greater C and energy were recovered in postprocess biomass compared to final fuels. However, differences between C$_4$ grasses were less prevalent. Critically, novel contrasts presented here between C$_4$ grasses and conversion pathways represent the utilization of structural lignocellulose—the most difficult to access plant-based polymer and a major limiting factor in biofuel and bioenergy production. Estimates of fuel values can also be augmented by the inclusion of nonstructural sugars and starches based on decided use. Nonstructural sugars could make overall C and energy recovery from sugar-producing grasses more competitive and will be investigated in future system analyses. The estimation of ethanol production could also be improved by process steps that better utilize hemicelluloses, which is a current research gap. However, unless a more efficient liquid fuel is produced, the low C and energy content of ethanol will limit the recovery of C and energy by HWP-EH compared to methane produced by AD.

In both pathways, most recovered energy remained in postprocess biomass instead of fuels. Though energy recovery in methane approached half of the energy recoverable in fuels and postprocess biomass, only a fraction of harvestable energy was recovered in ethanol. The inclusion of postprocess biomass and scaling fuel yield to represent the agricultural production area highlight the utilization of postprocess biomass as a key design consideration for an agricultural biorefinery system. Although there are research gaps in several process streams that must be resolved with future work, including hemicelluloses degraded during HWP, as well as CO$_2$ and digestate produced during AD, our data provide initial limitations to guide biorefinery system design. How well agricultural and biorefinery systems function within these C and energy constraints will determine if these biofuel

and bioenergy production systems are net C sources or sinks to the atmosphere. Future work to resolve several process streams and create data-driven models of the combined agricultural production and biorefinery system will inform sustainable development in the tropics using these crops and bioenergy pathways.

Author Contributions: Conceptualization, J.M.W., S.E.C., S.K.K., S.T., A.H., J.K., and N.M.; Formal analysis, J.M.W.; Funding acquisition, S.E.C., A.H., and J.K.; Investigation, J.M.W.; Methodology, J.M.W.; Project administration, S.E.C. and A.H.; Resources, S.E.C., S.K.K., S.T., and A.H.; Supervision, S.E.C., S.K.K., and S.T.; Visualization, J.M.W.; Writing—original draft, J.M.W.; Writing—review and editing, J.M.W., S.E.C., S.K.K., S.T., A.H., J.K., and N.M. All authors have read and agreed to the published version of the manuscript.

Institutional Review Board Statement: Not applicable.

Informed Consent Statement: Not applicable.

Data Availability Statement: Please contact corresponding author.

Conflicts of Interest: The authors declare no conflict of interest.

References

1. Pretty, J.; Bharucha, Z.P. Sustainable intensification in agricultural systems. *Ann. Bot.* **2014**, *114*, 1571–1596. [CrossRef]
2. Popp, J.; Lakner, Z.; Harangi-Rákos, M.; Fári, M. The effect of bioenergy expansion: Food, energy, and environment. *Renew. Sustain. Energy Rev.* **2014**, *32*, 559–578. [CrossRef]
3. Palm, C.; Blanco-Canqui, H.; DeClerck, F.; Gatere, L.; Grace, P. Conservation agriculture and ecosystem services: An overview. *Agric. Ecosyst. Environ.* **2014**, *187*, 87–105. [CrossRef]
4. Anderson-Teixeira, K.J.; Masters, M.D.; Black, C.K.; Zeri, M.; Hussain, M.Z.; Bernacchi, C.J.; DeLucia, E.H. Altered Belowground Carbon Cycling Following Land-Use Change to Perennial Bioenergy Crops. *Ecosystems* **2013**, *16*, 508–520. [CrossRef]
5. Sumiyoshi, Y.; Crow, S.E.; Litton, C.M.; Deenik, J.L.; Taylor, A.D.; Turano, B.; Ogoshi, R. Belowground impacts of perennial grass cultivation for sustainable biofuel feedstock production in the tropics. *GCB Bioenergy* **2017**, *9*, 694–709. [CrossRef]
6. Crow, S.E.; Deem, L.M.; Wells, J.M.; Sierra, C.A. Belowground carbon dynamics in tropical perennial C_4 grass agroecosystems. *Front. Environ. Sci.* **2018**, *6*, 18. [CrossRef]
7. Crow, S.E.; Wells, J.M.; Sierra, C.A.; Youkhana, A.H.; Ogoshi, R.M.; Richardson, D.; Tallamy Glazer, C.; Meki, M.N.; Kiniry, J.R. Carbon flow through energycane agroecosystems established post-intensive agriculture. *GCB Bioenergy* **2020**, *12*, 806–817. [CrossRef]
8. Qin, Z.; Dunn, J.B.; Kwon, H.; Mueller, S.; Wander, M.M. Soil carbon sequestration and land use change associated with biofuel production: Empirical evidence. *GCB Bioenergy* **2016**, *8*, 66–80. [CrossRef]
9. Powers, J.S.; Corre, M.D.; Twine, T.E.; Veldkamp, E. Geographic bias of field observations of soil carbon stocks with tropical land-use changes precludes spatial extrapolation. *Proc. Natl. Acad. Sci. USA* **2011**, *108*, 6318–6322. [CrossRef]
10. Morgan, T.J.; Youkhana, A.; Turn, S.Q.; Ogoshi, R.; Garcia-Pérez, M. Review of Biomass Resources and Conversion Technologies for Alternative Jet Fuel Production in Hawai'i and Tropical Regions. *Energy Fuels* **2019**, *33*, 2699–2762. [CrossRef]
11. Wells, J.M.; Crow, S.E.; Ogoshi, R.; Turano, B.; Hashimoto, A. Optimizing feedstock selection for biofuel production in Hawaii: CuO oxidative lignin products in C_4 grasses. *Biomass Bioenergy* **2015**, *83*, 511–515. [CrossRef]
12. Surendra, K.; Ogoshi, R.; Zaleski, H.M.; Hashimoto, A.G.; Khanal, S.K. High yielding tropical energy crops for bioenergy production: Effects of plant components, harvest years and locations on biomass composition. *Bioresour. Technol.* **2018**, *251*, 218–229. [CrossRef] [PubMed]
13. State of Hawaii; U.S. Department of Energy. Hawaii Clean Energy Initiative. Available online: http://www.hawaiicleanenergyinitiative.org (accessed on 12 March 2017).
14. State of Hawaii Office of Planning. *Feasibility and Implications of Establishing a Carbon Offset Program for the State of Hawaii*; State of Hawaii Office of Planning: Honolulu, HI, USA, 2019.

15. Searchinger, T.; Heimlich, R.; Houghton, R.A.; Dong, F.; Elobeid, A.; Fabiosa, J.; Tokgoz, S.; Hayes, D.; Yu, T.-H. Use of U.S. Croplands for Biofuels Increases Greenhouse Gases through Emissions from Land-Use Change. *Science* **2008**, *319*, 1238. [CrossRef]
16. Cherubini, F.; Bird, N.D.; Cowie, A.; Jungmeier, G.; Schlamadinger, B.; Woess-Gallasch, S. Energy- and greenhouse gas-based LCA of biofuel and bioenergy systems: Key issues, ranges and recommendations. *Resour. Conserv. Recycl.* **2009**, *53*, 434–447. [CrossRef]
17. Wyman, C.E.; Dale, B.E.; Elander, R.T.; Holtzapple, M.; Ladisch, M.R.; Lee, Y.Y. Coordinated development of leading biomass pretreatment technologies. *Bioresour. Technol.* **2005**, *96*, 1959–1966. [CrossRef] [PubMed]
18. Youkhana, A.H.; Ogoshi, R.M.; Kiniry, J.R.; Meki, M.N.; Nakahata, M.H.; Crow, S.E. Allometric Models for Predicting Above-ground Biomass and Carbon Stock of Tropical Perennial C$_4$ Grasses in Hawaii. *Front. Plant Sci.* **2017**, *8*, 650. [CrossRef]
19. Vanessa, S.S.; Sebastian, M.; Kerstin, S.; Jens, H.; Sebastian, W.; Klaus, M.; Kurt, M.; Wilhelm, C.; Simone, G.-H. Biomass and Biogas Yield of Maize (*Zea mays* L.) Grown under Artificial Shading. *Agriculture* **2018**, *8*, 178. [CrossRef]
20. Venuto, B.; Kindiger, B. Forage and biomass feedstock production from hybrid forage sorghum and sorghum–sudangrass hybrids. *Grassl. Sci.* **2008**, *54*, 189–196. [CrossRef]
21. Surendra, K.C.; Khanal, S.K. Effects of crop maturity and size reduction on digestibility and methane yield of dedicated energy crop. *Bioresour. Technol.* **2015**, *178*, 187–193. [CrossRef] [PubMed]
22. Mok, W.S.L.; Antal, M.J. Uncatalyzed solvolysis of whole biomass hemicellulose by hot compressed liquid water. *Ind. Eng. Chem. Res.* **1992**, *31*, 1157–1161. [CrossRef]
23. Laser, M.; Schulman, D.; Allen, S.G.; Lichwa, J.; Antal, M.J.; Lynd, L.R. A comparison of liquid hot water and steam pretreatments of sugar cane bagasse for bioconversion to ethanol. *Bioresour. Technol.* **2002**, *81*, 33–44. [CrossRef]
24. Mosier, N.; Hendrickson, R.; Ho, N.; Sedlak, M.; Ladisch, M.R. Optimization of pH controlled liquid hot water pretreatment of corn stover. *Bioresour. Technol.* **2005**, *96*, 1986–1993. [CrossRef]
25. Pérez, J.A.; Ballesteros, I.; Ballesteros, M.; Sáez, F.; Negro, M.J.; Manzanares, P. Optimizing Liquid Hot Water pretreatment conditions to enhance sugar recovery from wheat straw for fuel-ethanol production. *Fuel* **2008**, *87*, 3640–3647. [CrossRef]
26. Alvira, P.; Tomás-Pejó, E.; Ballesteros, M.; Negro, M.J. Pretreatment technologies for an efficient bioethanol production process based on enzymatic hydrolysis: A review. *Bioresour. Technol.* **2010**, *101*, 4851–4861. [CrossRef]
27. Wells, J.M.; Drielak, E.; Surendra, K.C.; Kumar Khanal, S. Hot water pretreatment of lignocellulosic biomass: Modeling the effects of temperature, enzyme and biomass loadings on sugar yield. *Bioresour. Technol.* **2020**, *300*, 122593. [CrossRef] [PubMed]
28. Bhagia, S.; Dhir, R.; Kumar, R.; Wyman, C.E. Deactivation of Cellulase at the Air-Liquid Interface Is the Main Cause of Incomplete Cellulose Conversion at Low Enzyme Loadings. *Sci. Rep.* **2018**, *8*, 1350. [CrossRef] [PubMed]
29. Alvira, P.; Negro, M.J.; Ballesteros, M. Effect of endoxylanase and α-l-arabinofuranosidase supplementation on the enzymatic hydrolysis of steam exploded wheat straw. *Bioresour. Technol.* **2011**, *102*, 4552–4558. [CrossRef]
30. Kumar, R.; Hu, F.; Sannigrahi, P.; Jung, S.; Ragauskas, A.J.; Wyman, C.E. Carbohydrate derived-pseudo-lignin can retard cellulose biological conversion. *Biotechnol. Bioeng.* **2013**, *110*, 737–753. [CrossRef]
31. Fu, N.; Peiris, P.; Markham, J.; Bavor, J. A novel co-culture process with Zymomonas mobilis and Pichia stipitis for efficient ethanol production on glucose/xylose mixtures. *Enzym. Microb. Technol.* **2009**, *45*, 210–217. [CrossRef]
32. Pereira, R.D.; Badino, A.C.; Cruz, A.J.G. Assessing the Performance of Industrial Ethanol Fermentation Unit Using Neural Networks. In *Computer Aided Chemical Engineering*; Friedl, A., Klemeš, J.J., Radl, S., Varbanov, P.S., Wallek, T., Eds.; Elsevier: Amsterdam, The Netherlands, 2018; Volume 43, pp. 175–180.
33. R Core Team. *R: A Language and Environment for Statistical Computing*; R Core Team: Vienna, Austria, 2020.
34. Patel, A.; Shah, A.R. Integrated lignocellulosic biorefinery: Gateway for production of second generation ethanol and value added products. *J. Bioresour. Bioprod.* **2021**. [CrossRef]
35. Medrano-García, J.D.; Ruiz-Femenia, R.; Caballero, J.A. Revisiting Classic Acetic Acid Synthesis: Optimal Hydrogen Consumption and Carbon Dioxide Utilization. In *Computer Aided Chemical Engineering*; Kiss, A.A., Zondervan, E., Lakerveld, R., Özkan, L., Eds.; Elsevier: Amsterdam, The Netherlands, 2019; Volume 46, pp. 145–150.
36. Cayuela, M.L.; Oenema, O.; Kuikman, P.J.; Bakker, R.R.; Van Groenigen, J.W. Bioenergy by-products as soil amendments? Implications for carbon sequestration and greenhouse gas emissions. *GCB Bioenergy* **2010**, *2*, 201–213. [CrossRef]
37. Kim, D. Physico-Chemical Conversion of Lignocellulose: Inhibitor Effects and Detoxification Strategies: A Mini Review. *Molecules* **2018**, *23*, 309. [CrossRef] [PubMed]
38. Patzek, T.W. Thermodynamics of the Corn-Ethanol Biofuel Cycle. *Crit. Rev. Plant Sci.* **2004**, *23*, 519–567. [CrossRef]
39. Patzek, T.W.; Pimentel, D. Thermodynamics of Energy Production from Biomass. *Crit. Rev. Plant Sci.* **2005**, *24*, 327–364. [CrossRef]
40. Naik, S.N.; Goud, V.V.; Rout, P.K.; Dalai, A.K. Production of first and second generation biofuels: A comprehensive review. *Renew. Sustain. Energy Rev.* **2010**, *14*, 578–597. [CrossRef]
41. Fivga, A.; Speranza, L.G.; Branco, C.M.; Ouadi, M.; Hornung, A. A review on the current state of the art for the production of advanced liquid biofuels. *Aims Energy* **2019**, *7*, 46–76. [CrossRef]